RSC Advances

ROYAL SOCIETY OF CHEMISTRY

www.rsc.org/advances

Facile chemical solution deposition of nanocrystalline CrN thin films with low magnetoresistance

Zhenzhen Hui,[a] Xianwu Tang,[a] Renhuai Wei,[a] Ling Hu,[a] Jie Yang,[a] Hongmei Luo,[b] Jianming Dai,[a] Wenhai Song,[a] Xingzhao Liu,[c] Xuebin Zhu,[*a] and Yuping Sun,[*a,d]

Received Xth XXXXXXXXXX 20XX, Accepted Xth XXXXXXXXX 20XX

First published on the web Xth XXXXXXXXXX 200X

DOI: 10.1039/b000000x

CrN thin films are first prepared by a facile chemical solution deposition method. The results show that the derived CrN thin films are nanocrystalline with the grain size of 30-60 nm. X-ray photoelectron spectroscopy measurement shows the stoichiometry of the derived thin film. The temperature dependent resistivity within the range of 2-300 K shows a semiconductor-like behavior with $d\rho/dT < 0$ and a discontinuity in resistivity at 253 K is observed due to the antiferromagnetic transition. At 10 K the magnetoresistance is as low as -0.06%under 45 kOe. The first growth of CrN thin films by the facile chemical solution deposition will provide an alternative route to prepare CrN thin films, especially for large-area CrN thin films with low-cost.

1 Introduction

Chromium nitride (CrN) has a lot of important applications such as hard coatings due to the high hardness, protective coatings due to the good corrosion resistance[1, 2, 3] and as a type of electronic or spintronic material due to the magnetic ordering.[4] In recently, it is reported that CrN thin films can be used as temperature sensors in high magnetic fields due to low magnetic-induced errors.[5]

Up to now, several methods have been successfully used to prepare CrN thin films including pulsed laser deposition,[6, 7] sputtering[4, 8] and molecular beam epitaxy.[9] All of these methods are vacuum-based, which are high-cost and difficult to prepare large-area thin films. An alternative approach for the fabrication of CrN thin films is the chemical solution deposition (CSD) method, which offers advantages in terms of cost, setup, and the ability to coat large areas.[10] However, there has no report about preparation of CrN thin films by CSD method. Additionally, it is difficult to prepare stoichiometric CrN due to the difficulties in control of the Cr and N content.

In this communication, CrN thin films are first prepared by a facile CSD method. The results show that the derived thin films are nanocrystalline with stoichiometry. The transport properties are investigated and a very low magnetoresistance (-0.06%) at 10 K under a magnetic field up to 45 kOe is observed. The results will provide a facile route to prepare CrN thin films with low-cost.

2 Experimental details

CrN thin films were prepared by a facile CSD method. The chromium nitrate ($Cr(NO_3)_3{\cdot}9H_2O$) was dissolved into the mixed solution of ammonia water and acetic acid with the solution concentration of 0.2 mol/L. Thin films were deposited on $LaAlO_3$ (001) single crystal substrates by the spin coating method. After spin coating, the thin films were baked under air atmosphere. In order to enhance the thickness, the above processes were repeated for eight times. Finally, the baked thin films were pyrolyzed in a forming gas (4% H_2 and 96% N_2) at 500 ˚ C, and then annealed in the flowing ammonia gas at 900 ˚ C with the heating ramp rate of 10 ˚ C/min. The thickness of the derived thin films is about 56 nm, indicating a thickness of 7 nm for each spin coating step. The processing flow chart is shown in the Figure 1. It should be pointed out that even the rapid thermal annealing processing was used to prepare the CrN thin films on the $LaAlO_3$ (001) single crystal substrates, the derived thin films were also polycrystalline, which could be attributed to the large lattice mismatch as discussed below.

X-ray diffraction (XRD) using a Philips X'pert Pro diffractometer with Cu K_α radiation was used to check the crystal structures. A field-emission scanning electronic microscopy (FEI Sirion 200 type, FEI, Hillsboro, OR) was used to detect the surface morphology. The crystallite size and the interface were checked by a transmission electron microscopy (TEM) inspection (JEM-2010, JEOL Ltd., Japan). The chemical states of Cr and N were analyzed using an X-ray photoelectron spectroscopy (XPS, ESCALAB250, Thermo, USA). The electrical transport properties were measured by a standard four-probe method on a Quantum Design physical property

[a] *Key Laboratory of Materials Physics, Institute of Solid State Physics, Chinese Academy of Sciences, Hefei 230031, PRC.*
[b] *Department of Chemical Engineering, New Mexico State University, Las Cruces, New Mexico 88003, US*
[c] *State Key Laboratory of Electronic Thin Films and Integrated Devices, University of Electronic Science and Technology of China, Chengdu 610054, PRC*
[d] *High Magnetic Field Laboratory, Chinese Academy of Sciences, Hefei 230031, PRC*
[*] Corresponding author: xbzhu@issp.ac.cn (Xuebin Zhu) ypsun@issp.ac.cn (Yuping Sun)

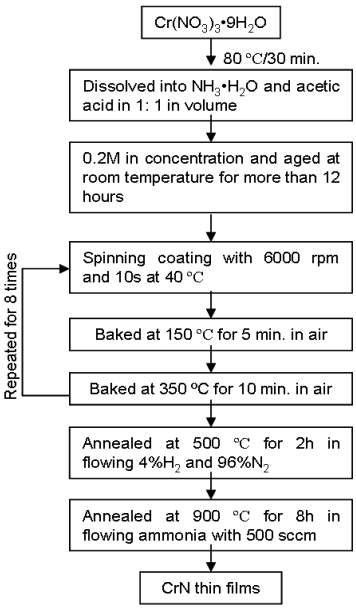

Fig. 1 Flow chart of preparation of CrN thin films by the facile CSD method.

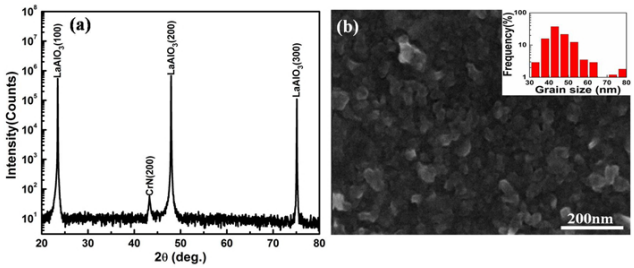

Fig. 2 (a) XRD pattern of the CrN thin film deposited on $LaAlO_3$ (100) single crystal substrate. (b) FE-SEM result for the CrN thin film and the inset is the history diagram of the grain size.

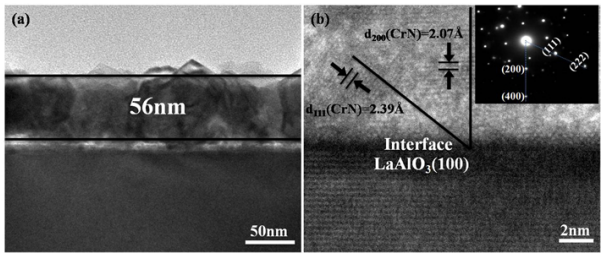

Fig. 3 (a) Cross-sectional TEM image and (b) cross-sectional high-resolution TEM image near the CrN/$LaAlO_3$ interface. The inset of (b) shows the corresponding selected area electron diffraction (SAED) pattern.

measurement system (PPMS) within the temperature range of 2–300 K and a magnetic field up to 45 kOe.

3 Results and discussion

Figure 2(a) shows the XRD result of the derived CrN thin film. Only one peak located at 2θ= 43.28 ° can be clearly seen within the measured 2θ range from 20 to 80 ° except for the diffraction peaks from the substrate, which can be attributed to the CrN (200) (PDF Card No.03-065-9001). It is seen that the XRD intensity of CrN (200) is about 60 counts. The relatively low XRD intensity of the derived CrN thin film maybe attributed to the small crystallite size of CrN grains and the low thickness value. The calculated lattice constant by the Bragg formula is 0.418 nm, which is same as previous reports.[11, 12] Additionally, the XRD rocking curve and in-plane Φ-scanning measurements show the characteristic of polycrystalline for the derived CrN thin film, which can be attributed to the large lattice mismatch ($\varepsilon = \frac{a_f - a_s}{a_f} \times 100\% = 9.33\%$, a_f and a_s is the lattice constant of the thin film and the substrate respectively) between the CrN thin film and the $LaAlO_3$ substrate (a=0.379 nm). Figure 2(b) shows the FE-SEM result of the derived CrN thin film. It is seen that the surface is relatively smooth and dense with the particle size of 30–60 nm as determined from the history diagram of the grain size, suggesting the good quality for the derived CrN thin film.

In order to further investigate the microstructures of the derived CrN thin film, TEM measurements are carried out and the results are shown in Figure 3. As shown in Figure 3(a), it is seen that the thickness is of 56 nm. From the high-resolution TEM image as shown in Figure 3(b), a relatively sharp interface between CrN/$LaAlO_3$ is observed, indicating almost no chemical reactions between the thin film and the single crystal substrate. Additionally, randomly oriented grains with blurred grain boundaries can be observed, which indicate that the derived CrN thin film is polycrystalline and the result is same as the XRD measurements. The d spacings as indexed in Figure 3(b) can be attributed to CrN (200) and CrN (111) planes. From the corresponding selected-area electron diffraction (SAED) as shown in the inset of Figure 3(b), the crystal structure of the derived CrN thin film can be indexed as face-center-cubic (fcc), which is same as previous report[13] and further confirms the successful achievements of CrN thin films.

To investigate the stoichiometry of the derived thin films, XPS measurements are performed and the results are shown in Figure 4. In Figure 4(a), it is seen that two peaks centered at 575.6 eV and 585.2 eV can be attributed to the Cr $2p_{3/2}$ and Cr $2p_{1/2}$, respectively. Additionally, the shapes of the Cr 2p peaks are asymmetric. It is usually observed that the transition-metal XPS spectra are asymmetric due to the Doniach-Sunjic equation.[14] It is suggested that a potential will be created between the hole left by the photoemission

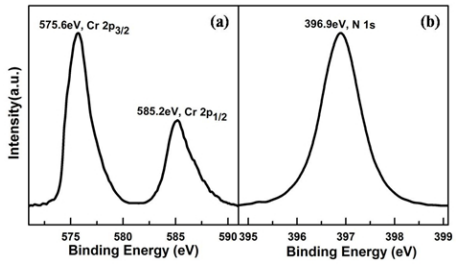

Fig. 4 XPS spectra of the derived CrN thin film (a) Cr2p and (b) N1s.

process and the remaining electrons, which permits the promotion of electrons near E_F to empty states just above it.[14] As a result, the XPS peak will be asymmetric and extends to higher binding energies. The asymmetric peaks have been also observed in CrN as previously reported.[15, 16] On the other hand, from Figure 4(b) it is seen that the peak centered at 396.9 eV can be attributed to the N 1s, which confirms that N atoms have reacted with Cr atoms to form CrN. In the previous reports,[15, 16] it is observed that the N content in CrN_x can be determined by the N 1s peak.With N content increasing, the binding energy of N 1s is decreased.[15, 17] For the stoichiometric CrN,[17] the binding energy of N 1s is 396.7eV,[18] which is nearly same as our experimental result. In fact, deconvolution processing for the Cr $2p_{3/2}$ peak has been carried out, and the result shows that the Cr^{3+} is more than 0.95 meaning that the N content is higher than 0.95 in the derived CrN thin film. Combined with the position of N 1s peak as well as the deconvolution of Cr $2p_{3/2}$ peak, it is safety to say that the derived CrN is at least nearly stoichiometric.

Figure 5(a) shows the temperature-dependent electrical resistivity of the derived CrN thin film. One can see that the derived thin film shows a semiconductor-like behavior with $d\rho/dT<0$ within the measured temperature range 2-300 K, which is same as the previous reports about CrN ceramics and CrN thin films.[4, 19, 20] The resistivity at 300 K is 4.0 mΩ·cm, which is within the wide range of the previously reported values (1.7 mΩ·cmto 3.5×10^{-1} Ω·cm) for the polycrystalline CrN powders and thin films.[7, 21, 22] Usually, in CrN ceramics and polycrystalline thin films a paramagnetic (with NaCl structure) to antiferromagnetic (orthorhombic P_{nma} structure) transition will be occurred at the Néel temperature T_N.[23, 24] At T_N, a discontinuity in resistivity will be observed. As shown in the inset of Figure 5(a), the discontinuity is occurred at 253K defined from the peak in $d\rho/dT$, which further confirms the successful preparation of CrN thin films by the facile chemical solution deposition.

Figure 5(b) shows the magnetic field dependent resistivity at different temperatures. It is seen that when the temperature is higher than the T_N such as 300 K the magnetoresistance MR

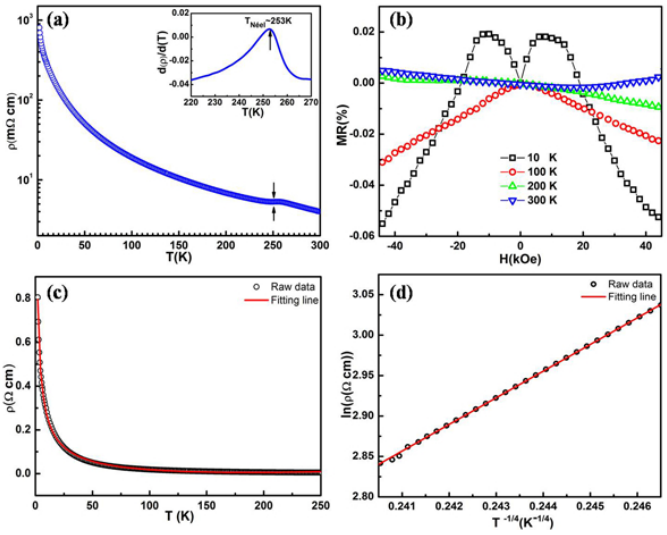

Fig. 5 (a) ρ-T result for the derived CrN thin film, and the inset shows the $d\rho/dT$ result to determine the T_N. (b) MR-H curves measured at different temperatures. (c) ρ-T fitting result at temperature of 2-250 K. (d) ρ-T fitting result at temperature of 270-300 K.

($=\frac{\rho_H-\rho_0}{\rho_H}\times100\%$, where ρ_H and ρ_0 is the resistivity with and without applied magnetic field) is positive within the range of the measured magnetic fields, which can be attributed to the induced Lorentz force by applying magnetic field.[25] With decreasing the temperature down to T_N such as at 200 K and 100 K, one can see that the MR is negative and the value is enhanced with decreasing the temperature, which is same as previous reports and can be attributed to the decreased carrier scattering due to the enhanced antiferromagnetic spin arrangement by applying magnetic field.[26, 27, 28, 29] Further to decrease the temperature to lower temperatures such as 10 K, it is clearly seen that a crossover from a positive MR at low fields to a negative MR at high fields is observed. Moreover, it is seen that the MR at 10 K is as low as -0.06% under 45 kOe, which is very small and maybe suitable to be used as temperature sensors in high magnetic fields.[5]

In order to investigate the electrical transport properties, the resistivity is fitted within different temperature ranges. It is found that the resistivity at temperature lower than T_N can be well fitted considering the weak localization, Coulomb interaction in antiferromagnetic phase and electron-electron scattering ($\rho=\rho_0+A\ln(x)+\frac{B}{\sqrt{x}}+Cx^2$, where ρ_0, A, B and C are constants).[30] Based on the fitting result, it is suggested that the crossover of MR at 10 K can be attributed to the weak delocalization at low magnetic fields and weak localization at higher magnetic fields.[31] On the other hand, the resistivity at the temperature of 270-300K can be well fitted by the three-dimensional variable-range-hopping (3D-VRD) model

($\rho = \rho_0 \exp(\frac{T_0}{T})^{1/4}$, where $\rho_0$and T_0 are constants) which is same as the previous reports.[32]

4 Conclusions

A facile chemical solution deposition was firstly developed to prepare CrN thin films. The results showed that the derived CrN thin films were polycrystalline, stoichiometry, and nanocrystalline with the grain size of 30-60 nm. The temperature dependent resistivity showed a semiconductor-like behavior with a discontinuity at 253 K due to the antiferromagnetic transition. A very low magnetoresistance (-0.06%) at 10 K under 45 kOe was observed, suggesting that the CrN thin films can be considered to be used as cryogenic temperature sensors. The successful preparation of CrN thin films by a facile chemical solution deposition will provide an alternative route to fabricate CrN thin films, especially for large-area applications.

This work was supported by the National Basic Research Program of China (2014CB931704) and by the National Nature Science Foundation of China under Contract Nos. 51171177 and 11174288.

References

1 I. Scanavino and M. Prencipe, RSC Advances, 2013, 3, 17813-17821.

2 M. H. Yang, R. Guarecuco and F. J. Disalvo, Chem. Mater., 2013, 25, 1783-1787.

3 S. P. Pujari, L. Scheres, B. V. Lagen and H. Zuilhof, Langmuir, 2013, 29, 10393-10404.

4 X. Y. Zhang, J. S. Chawla, R. P. Deng and D. Gall, Phys. Rev. B, 2011, 84, 073101.

5 K. Satoh, Y. Kakehi, M. Uno, Y. Sakurai, T. Yotsuya and T. Ishida, Jpn. J. Appl. Phys., 2012, 51, 01AC07.

6 J. M. Lackner, W. Waldhauser, M. Kahn, R. Berghauser, D. Hufnagel, R. Major, L. Major and B. Major, Plasma Process. Polym., 2007, 4, S906-S909.

7 K. Inumaru, K. Koyama, N. Imo-oka and S. Yamanaka, Phys. Rev. B, 2007, 75, 054416.

8 C. Heinisch, P. Ramminger and H. Hutter, Anal Bioanal Chem., 2002, 374, 592-596.

9 A. Ney, R. Rajaram, S. S. P. Parkin, T. Kammermeier and S. Dhar, Appl. Phys. Lett., 2006, 89, 112504.

10 G. Subramanyam, M. W. Cole, N. X. Sun, T. S. Kalkur, N. M. Sbrockey, G. S. Tompa, X. M. Guo, C. L. Chen, S. P. Alpay, G. A. Rossetti, Jr. K.Dayal, L. Q. Chen and D. G. Schlom, J. Appl. Phys., 2013, 114, 191301.

11 C. Constantin, M. B. Haider, D. Ingram and A. R. Smitha, Appl. Phys. Lett., 2004, 85, 6371.

12 D. Gall, C. S. Shin, T. Spila, M. Oden, M. J. H. Senna, J. E. Greene and I. Petrov, J. Appl. Phys., 2002, 91, 3589.

13 X. F. Duan, W. B. Mi, Z. B. Guo and H. L. Bai, J. Appl. Phys., 2013, 113, 023701.

14 E.Sacher, Langmuir, 2010, 26, 3807-3814.

15 M.Chen, S. Wang, J. Z. Zhang, D. W. He and Y. S. Zhao, Chem.Eur. J., 2012, 18, 15459-15463. 16 I. Bertoti, M. Mohai, P. H.

16 Mayrhofer, C. Mitterer, Surf. Interface Anal, 2002, 34,740-743.

17 C. Emerya, A. R. Chourasiaa and P. Yasharb, J. Electron.Spectrosc., 1999, 104, 91-97.

18 F. Rivadulla, M. Ba?obre-Lpez, C. X. Quintela, A. Pi?eiro, V. Pardo, D. Baldomir, M. A. Lpez-Quintela, J. Rivas, C. A. Ramos, H. Salva, J. S. Zhou and J. B. Goodenough, Nat. Mater., 2009, 8, 947-951.

19 P. S. Herle, M. S. Hegde, N. Y. Vasathacharya, S. Philip, M. V. R. Rao and T. Sripathi, J. Solid State Chem., 1997, 134, 120.

20 C. X. Quintela, F. Rivadulla and J. Rivas, Appl. Phys. Lett., 2009, 94, 152103.

21 P. A. Anderson, R. J. Kinsey, S. M. Durbin, M. Markwitz, J. Kennedy, A. Asadov, W. Gao and R. J. Reeves, J. Appl. Phys., 2005, 98, 043903.

22 R. Sanjines, O. Banakh, C. Rojas, P. E. Schmid and F. Levy, Thin Solid Films, 2002, 312, 420-421.

23 J. D. Browne, P. R. Liddell, R. Street and T. Mills, Phys. Status Solidi., 1970, 1, 715.

24 L. M. Corliss, N. Elliott and J. M. Hastings, Phys. Rev., 1960, 117,929.

25 X. F. Duan, W. B. Mi, Z. B. Guo and H. L. Bai, Acta Mater., 2012, 60, 3690-3697.

26 S. Hikami, A. I. Larkin and Y. Nagaoka, Prog. Theor. Phys., 1980, 63, 707-710.

27 G. Bergmann, Physics Reports, 1984, 107, 1-58.

28 P. E. Lindelof, J. Norregaard and J. B. Hansen, Condensed Matter, 1985, 59, 423-428.

29 S. Wang and P. E. Lindelof, J. Low Temp. Phys., 1988, 71, 403-444.

30 M. Suzuki and I. S. Suzuki, Phys. Rev. B, 1999, 61, 5013-5019.

31 M. E. Gershenzon, B. N. Gubankov and Y. E. Zhuravlev, Sov. Phys. JETP, 1982, 56, 1362-1369.

32 Y. Tsuchiya, K. Kosuge, Y. Ikeda, T. Shigematsu, S. Yamaguchi and N.Nakayama, Mater. Trans., 1996, 121, 37.